

A Two-Stage Isolated/Bidirectional Dc-Dc Converter

Vaddemoni Swarna Rekha

swarna.vaddemoni@gmail.com

Abstract: In this paper we proposed a two-stage isolated/bidirectional dc/dc converter with three bridges. In these two bridges for electrical isolation purpose and constant gain, and bidirectional control is accomplished through only a single bridge. Link capacitor can be alleviated by capacitor division and synchronizing operation of both stages and rms currents in the high voltage source. This construction provides a simple control scheme and removes snubber circuitry, so high efficiency can be obtained under a high switching frequency regardless of operational modes.

Keywords: voltage-fed full-bridge, Time-domain ripple

I. INTRODUCTION

Fuel cell has a slow dynamic response, so the power supply from the fuel cell cannot cope with the power demand during a transient load. Thus, a secondary power source is required to compensate the power difference between the fuel cell and the load, and a battery is generally used to supply a transient power. The power flow between the fuel cell and the battery is managed by a bidirectional dc/dc converter. Conventional isolated/bidirectional dc/dc converters for high-power applications have a voltage-fed full-bridge (FB) (VF-FB) scheme in the high-voltage (HV) side and various current-fed (CF) schemes in the low-voltage (LV) side in general because voltage-fed half-bridge (HB) and voltage-fed push-pull (PP) schemes have disadvantages of high current stress and/or high voltage stress. According to which schemes are used in the LV side, they have

several variations such as VF-FB + two-inductor CF-HB, VF-FB + CF-FB, and VF-FB + CF-PP with six or eight switches. These converters suffer from efficiency decrease at a light-load condition and low efficiency at boost-mode operation due to switching loss. Also, they require a snubber circuit such as an active-clamp circuit to alleviate turn-off voltage spikes in the LV side, which increases the switch number by one or two as a result. In this letter, a two-stage isolated/bidirectional dc/dc converter adopting a current ripple reduction technique is proposed. The resonant converter with two bridges takes in charge of electrical isolation and constant gain, and the bidirectional control is accomplished using only the second stage with a single bridge. To reduce rms currents in the HV source and link capacitor, capacitor division and synchronizing operation of two stages are adopted. A 2-kW prototype converter has been designed and verified based on design guidelines that are derived from the circuit analysis.

II. CHARACTERIZATION OF RIPPLE CURRENT

Ripple current refers to the AC portion of the current signal applied to a device in its application. Although this term defines an AC portion of the applied signal, it is usually in reference to the small level of variation of DC signals encountered in a power supply application. Ripple current ratings for capacitors can be somewhat arbitrary. Although the EIA has standards for calculating ripple current ratings, some manufactures use their own methods. This makes it difficult for

end customers to have a one-to-one comparison. This update is intended to educate the reader on the background of ripple current capabilities, and the variables that affect them. Ripple current is the rms value of alternating current flowing through a capacitor. This current causes an internal temperature rise due to power losses within the capacitor. The most common meaning of ripple in electrical science is the small unwanted residual periodic variation of the direct current (dc) output of a power supply which has been derived from an alternating current (ac) source. This ripple is due to incomplete suppression of the alternating waveform within the power supply. As well as this time-varying phenomenon, there is a frequency domain ripple that arises in some classes of filter and other signal processing networks. In this case the periodic variation is a variation in the insertion loss of the network against increasing frequency. The variation may not be strictly linearly periodic. In this meaning also, ripple is usually to be considered an unwanted effect, its existence being a compromise between the amount of ripple and other design parameters.

Time-domain ripple:

Ripple factor (γ) may be defined as the ratio of the root mean square (rms) value of the ripple voltage to the absolute value of the dc component of the output voltage, usually expressed as a percentage. However, ripple voltage is also commonly expressed as the peak-to-peak value. This is largely because peak-to-peak is both easier to measure on an oscilloscope and is simpler to calculate theoretically. Filter circuits intended for the reduction of ripple are usually called smoothing circuits.

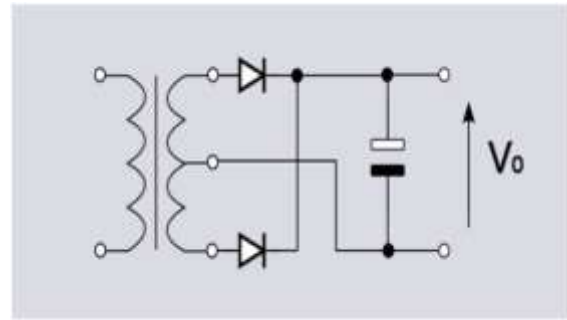


Fig.1: Simple filter circuit

Full-wave rectifier circuit with a reservoir capacitor on the output for the purpose of smoothing ripple the simplest scenario in ac to dc conversion is a rectifier without any smoothing circuitry at all. The ripple voltage is very large in this situation; the peak-to-peak ripple voltage is equal to the peak ac voltage. A more common arrangement is to allow the rectifier to work into a large smoothing capacitor which acts as a reservoir. After a peak in output voltage the capacitor (C) supplies the current to the load (R) and continues to do so until the capacitor voltage has fallen to the value of the now rising next half-cycle of rectified voltage. At that point the rectifiers turn on again and deliver current to the reservoir until peak voltage is again reached. If the time constant, CR, is large in comparison to the period of the ac waveform, then a reasonably accurate approximation can be made by assuming that the capacitor voltage falls linearly. A further useful assumption can be made if the ripple is small compared to the dc voltage. In this case the phase angle through which the rectifiers conduct will be small and it can be assumed that the capacitor is discharging all the way from one peak to the next with little loss of accuracy.

With the above assumptions the peak-to-peak ripple voltage can be calculated as:

For a full-wave rectifier:

$$V_{pp} = \frac{I}{2fC}$$

For a half-wave rectification:

$$V_{pp} = \frac{I}{fC}$$

Where

V_{pp} is the peak-to-peak ripple voltage

I is the current in the circuit

f is the frequency of the ac power

C is the capacitance

For the rms value of the ripple voltage, the calculation is more involved as the shape of the ripple waveform has a bearing on the result. Assuming a saw tooth waveform is a similar assumption to the ones above and yields the result

where

γ is the ripple factor

R is the resistance of the load

Another approach to reducing ripple is to use a series choke. A choke has a filtering action and consequently produces a smoother waveform with less high-order harmonics. Against this, the dc output is close to the average input voltage as opposed to the higher voltage with the reservoir capacitor which is close to the peak input voltage. With suitable approximations, the ripple factor is given by:

Where

ω is the angular frequency

L is the inductance of the choke

More complex arrangements are possible; the filter can be an LC ladder rather than a simple choke or the filter and the reservoir capacitor can both be used to gain the benefits of both. The most commonly seen of these is a low-pass Π -filter consisting of a reservoir capacitor followed by a series choke followed by a further shunt capacitor.[5] However, use of chokes is deprecated in contemporary designs for economic reasons. A more common

solution where good ripple rejection is required is to use a reservoir capacitor to reduce the ripple to something manageable and then pass through a voltage regulator circuit. The regulator circuit, as well as regulating the output, will incidentally filter out nearly all of the ripple as long as the minimum level of the ripple waveform does not go below the voltage being regulated to.

The majority of power supplies are now switched mode. The filtering requirements for such power supplies are much easier to meet owing to the frequency of the ripple waveform being very high. In traditional power supply designs the ripple frequency is either equal to (half-wave), or twice (full-wave) the ac line frequency. With switched mode power supplies the ripple frequency is not related to the line frequency, but is instead related to the frequency of the chopper circuit.

III. SYSTEM STUDY

A. Operation of DC-DC converter

In its simplest form, a DC-DC converter simply uses resistors as needed to break up the flow of incoming energy – this is called linear conversion. However, linear conversion is a wasteful process which unnecessarily dissipates energy and can lead to overheating. A more complex, but more efficient, manner of DC-DC conversion is switched-mode conversion, which operates by storing power, switching off the flow of current, and restoring it as needed to provide a steadily modulated flow of electricity corresponding to the circuit's requirements. This is far less wasteful than linear conversion, saving up to 95% of otherwise wasted energy.

B. Types of DC-DC Converters

DC-DC converters can vary widely in size, usage, and the level of voltage processed. In

the 1970's, conventional PWM power converters were operated in a switched mode operation. Power switches have to cut off the load current within the turn-on and turn-off times under the hard switching conditions. Hard switching refers to the stressful switching behavior of the power electronic devices. The switching trajectory of a hard-switched power device is shown in Fig.1. During the turn-on and turn-off processes, the power device has to withstand high voltage and current simultaneously, resulting in high switching losses and stress. Dissipative passive snubbers are usually added to the power circuits so that the dv/dt and di/dt of the power devices could be reduced, and the switching loss and stress be diverted to the passive snubber circuits. However, the switching loss is proportional to the switching frequency, thus limiting the maximum switching frequency of the power converters. Because the switching loss and stress have been reduced, soft-switched converter can be operated at the very high frequency (typically 500kHz to a few Mega-Hertz).

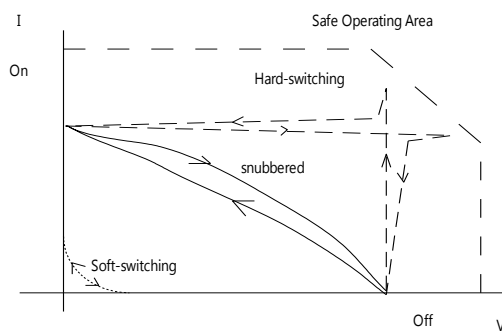


Fig.2 Typical switching trajectories of power switches.

Soft-switching converters also provide an effective solution to suppress EMI and have been applied to DC-DC, AC-DC and DC-AC converters. This chapter covers the basic technology of resonant and soft-switching converters.

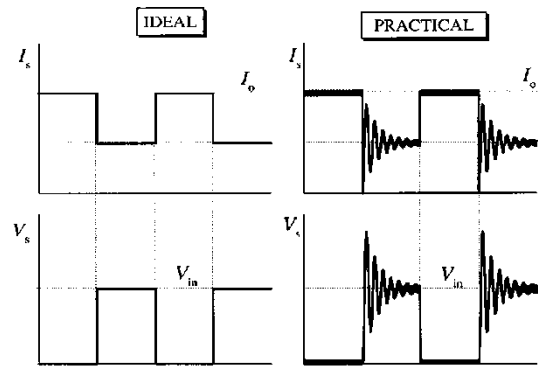


Fig.3. Typical switching waveforms of (a) hard-switched and (b) Soft-switched devices

Various forms of soft-switching techniques such as ZVS, ZCS, voltage clamping, zero transition methods etc. are addressed. The emphasis is placed on the basic operating principle and practicality of the converters without using much mathematical analysis.

II. PROPOSED CONVERTER

Description of the Proposed Converter is mentioned in this section. Figs. 3 and 4 show the proposed converter with key waveforms, and its operational mode diagrams are shown in Fig. 5. The resonant converter with a fixed frequency automatically forms bidirectional power flow according to input/output conditions, and the bidirectional control is accomplished using only M5 and M6.

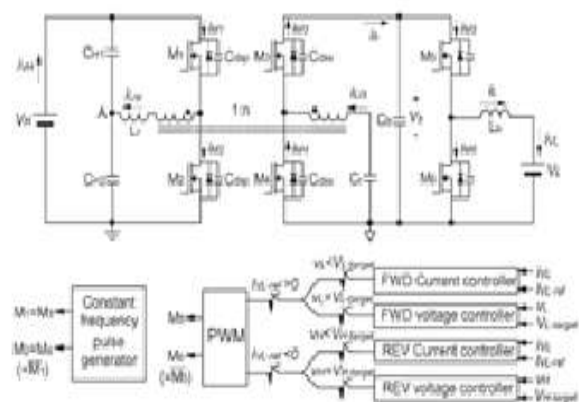


Fig.4: Schematic of the proposed converter

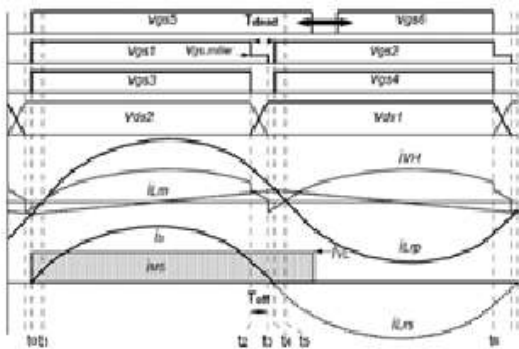


Fig. 5: Operational waveforms of the proposed converter

The bulk capacitors CH1 and CH2 provide resonant current paths to alleviate the current ripple from the HV source. The voltage-doubler structure in the LV side reduces the rms current of the link capacitor Cb by compensating the discharge current, which helps to reduce the link capacitor size. Before explanation, CH1 and CH2 have the same value, and the resonant frequency fr is equal to the switching frequency fs.

Also, the second stage is modeled by a pulse current source with the switching frequency synchronized with that of the first stage. Because the resonant converter has a symmetric structure, buck and boost modes have identical operation, and we will explain the operation only with buck mode. When M1 and M3 are turned on at t0, M1 has zero-voltage switching (ZVS), and the secondary resonant current iLrs begins to flow through the channel of M3, the link capacitor Cb, and the resonant capacitor Cr. After the primary resonant current iLrp crosses zero at t1, it flows through the channel of M1 and the resonant inductor Lr. Because the impedances seen from node A to CH1 and CH2 are identical, iLrp is divided into half, and each half current flows through the two capacitors. When vgs1 is decreased to the Miller plateau voltage Vgs,Miller at t2, the drain-source voltage of M1 vds1 is linearly

increased, and iLrs flows through the body diode of M3. The discharge current of the drain-source capacitance of M2 Cdsp can be written as $iM2 = -CdspVH/Toff$, where Toff is the turn-off time of M1. Thus, the HV-side current iVH becomes $iLrp/2 - CdspVH/Toff$. After M1 is completely turned off at t3, iLrp starts to flow through the body diode of M2, and the ON state of the body diode of M3 is maintained to provide the current path of iLrs. When M2 and M4 are turned on at t4, ZVS of M2 is accomplished, and iLrs flows through the channel of M4 and Cr. After t5, iLrp changes its direction, flowing through CH1 and CH2 similar to mode 2. Thus, iVH also has iLrp/2. Referring to the key waveforms, the current ripple in the HV source is like that of the FB structure, and the charge and discharge currents of Cb happen at the same time. The current cancellation helps to reduce the rms current of Cb that suffers from the heavy current stress. In steady state, the average discharge current of Cb, which is equal to the average LV-side current IVL, is balanced with the average charge current so that iLrs can be written as $iLrs = \pi DIVL \sin(2\pi frt)$, where D is the duty ratio of M5. Because the magnetizing current iLm is circulated in the primary side, the effective current supplied from the HV source is equal to half the rectified current iLrs reflected to the primary side, i.e., $iVH = |\pi DIVL \sin(2\pi frt)/2|$. By averaging this equation, the current gain becomes $IVH = nDIVL$, and it follows that the voltage gain is derived as $VL = nDVH$. Thus, the bidirectional power flow is controlled only with D.

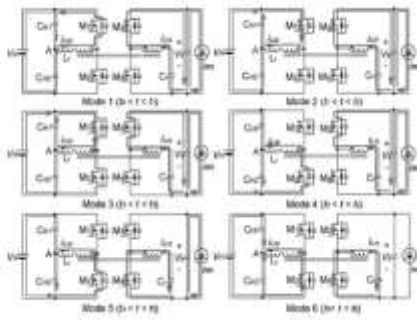


Fig. 3: Operational mode diagrams

Fig.6: Proposed converter circuit diagram

However, the proposed converter has drawbacks in capacitor blocks and diode blocks due to the cascaded structure of two converters. Synthesizing the comparisons, the structure of the proposed converter is not inferior to the conventional converters despite the two-stage structure.

IV. SIMULATION RESULTS

A two stage isolated bidirectional DC/DC Converter for PV connections is modeled and simulated using the MATLAB.

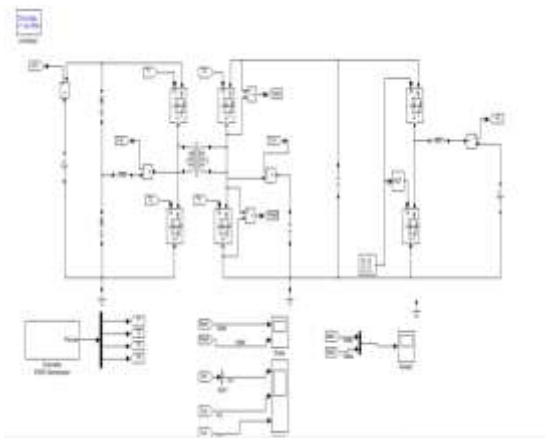


Fig: 6.1 Simulation diagram for proposed converter

The MATLAB model of A bidirectional DC/DC Converter is shown in the Fig 6.1. The fig 6.2 shows that the output waveforms of i_{VL} & i_{VH} and V_{ds1} & V_{ds2} .

Bidirectional DC/DC Converter:

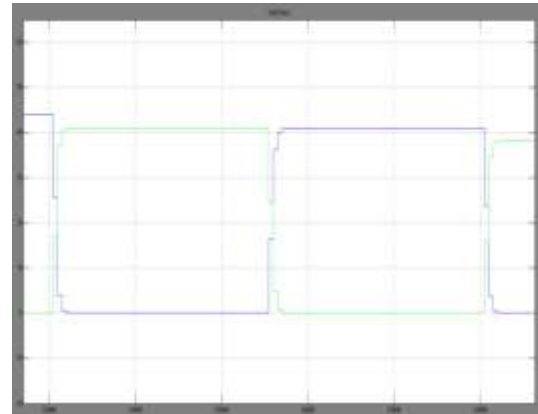


Fig: 6.2 Outputs of V_{ds1} & V_{ds2}

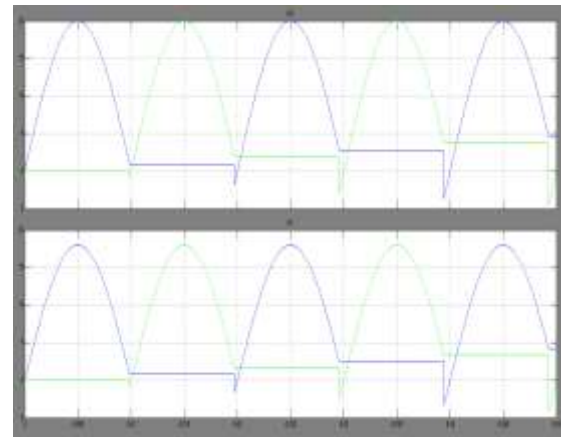


Fig: 6.3 Output Waveforms of i_{VH} & i_{VL}

Simulation diagram of proposed converter with PV Cell:

The below figure shows the isolated bidirectional DC/DC Converter in which the input is replace by a PV cell.

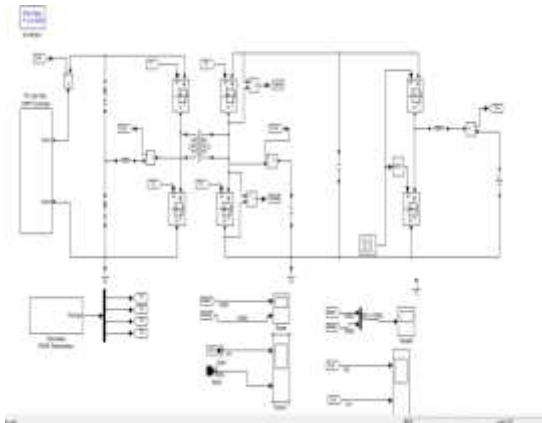


Fig: 6.4 Simulation diagram of proposed converter with PV Cell

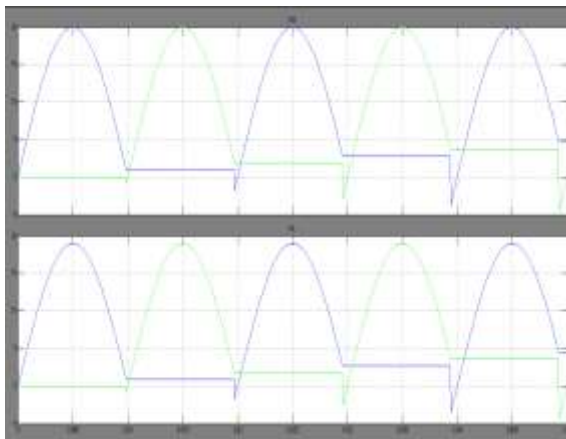


Fig: 6.5 Output waveforms of i_{VH} & i_{VL}

V. CONCLUSION

Simulation of the proposed model is presented in the section.IV. The analysis of the two-stage isolated/bidirectional dc/dc converter with three bridges produced better response in terms of many electrical characteristics than the contemporaray and conventional ones.

REFERENCES

[1] B. Goll and H. Zimmermann, "A comparator with reduced delay time in 65-nm CMOS for supply voltages down to 0.65," *IEEE Trans. Circuits Syst. II, Exp. Briefs*, vol. 56, no. 11, pp. 810–814, Nov. 2009.

[2] S. U. Ay, "A sub-1 volt 10-bit supply boosted SAR ADC design instandard CMOS," *Int. J. Analog Integr. Circuits Signal Process.*, vol. 66, no. 2, pp. 213–221, Feb. 2011.

[3] A. Mesgarani, M. N. Alam, F. Z. Nelson, and S. U. Ay, "Supplyboosting technique for designing very low-voltage mixed-signal circuits in standard CMOS," in *Proc. IEEE Int. Midwest Symp. Circuits Syst. Dig. Tech. Papers*, Aug. 2010, pp. 893–896.

[4] B. J. Blalock, "Body-driving as a Low-Voltage Analog Design Technique for CMOS technology," in *Proc. IEEE Southwest Symp. Mixed-Signal Design*, Feb. 2000, pp. 113–118.

[5] M. Maymandi-Nejad and M. Sachdev, "1-bit quantiser with rail to rail input range for sub-1V ??modulators," *IEEE Electron. Lett.*, vol. 39, no. 12, pp. 894–895, Jan. 2003.

[6] Y. Okaniwa, H. Tamura, M. Kibune, D. Yamazaki, T.-S. Cheung, J. Ogawa, N. Tzartzanis, W. W. Walker, and T. Kuroda, "A 40G-b/s CMOS clocked comparator with bandwidth modulation technique," *IEEE J. Solid-State Circuits*, vol. 40, no. 8, pp. 1680–1687, Aug. 2005.

[7] B. Goll and H. Zimmermann, "A 0.12 μm CMOS comparator requiring 0.5V at 600MHz and 1.5V at 6 GHz," in *Proc. IEEE Int. Solid-State Circuits Conf., Dig. Tech. Papers*, Feb. 2007, pp. 316–317.

[8] B. Goll and H. Zimmermann, "A 65nm CMOS comparator with modified latch to achieve 7GHz/1.3mW at 1.2V and 700MHz/47 μW at 0.6V," in *Proc. IEEE Int. Solid-State Circuits Conf. Dig. Tech. Papers*, Feb. 2009, pp. 328–329.

- [9] B. Goll and H. Zimmermann, "Low-power 600MHz comparator for 0.5 V supply voltage in 0.12 μm CMOS," IEEE Electron. Lett., vol. 43, no. 7, pp. 388–390, Mar. 2007.
- [10] D. Shinkel, E. Mensink, E. Klumperink, E. van Tuijl, and B. Nauta, "A double-tail latch-type voltage sense amplifier with 18ps Setup+Hold time," in Proc. IEEE Int. Solid-State Circuits Conf., Dig. Tech. Papers, Feb. 2007, pp. 314–315.
- [11] P. Nuzzo, F. D. Bernardinis, P. Terreni, and G. Van der Plas, "Noise analysis of regenerative comparators for reconfigurable ADC architectures," IEEE Trans. Circuits Syst. I, Reg. Papers, vol. 55, no. 6, pp. 1441–1454, Jul. 2008.
- [12] A. Nikoozadeh and B. Murmann, "An analysis of latched comparator offset due to load capacitor mismatch," IEEE Trans. Circuits Syst. II, Exp. Briefs, vol. 53, no. 12, pp. 1398–1402, Dec. 2006.
- [13] S. Baban-Mashhadi and R. Lotfi, "An offset cancellation technique for comparators using body-voltage trimming," Int. J. Analog Integr. Circuits Signal Process., vol. 73, no. 3, pp. 673–682, Dec. 2012.
- [14] J. He, S. Zhan, D. Chen, and R. J. Geiger, "Analyses of static and dynamic random offset voltages in dynamic comparators," IEEE Trans. Circuits Syst. I, Reg. Papers, vol. 56, no. 5, pp. 911–919, May 2009.
- [15] J. Kim, B. S. Leibowitz, J. Ren, and C. J. Madden, "Simulation and analysis of random decision errors in clocked comparators," IEEE Trans. Circuits Syst. I, Reg. Papers, vol. 56, no. 8, pp. 1844–1857, Aug. 2009.
- [16] P. M. Figueiredo and J. C. Vital, "Kickback noise reduction technique for CMOS latched comparators," IEEE Trans. Circuits Syst. II, Exp. Briefs, vol. 53, no. 7, pp. 541–545, Jul. 2006.
- [17] B. Wicht, T. Nirschl, and D. Schmitt-Landsiedel, "Yield and speed optimization of a latch-type voltage sense amplifier," IEEE J. Solid-State Circuits, vol. 39, no. 7, pp. 1148–1158, Jul. 2004.
- [18] D. Johns and K. Martin, Analog Integrated Circuit Design, New York, USA: Wiley, 1997.

Author Profile:



Vaddemoni Swarna Rekha completed M.E. with specialization in power electronic systems. My Areas of Interest are Power flow control in drives, operation and control of machines.